



Investigations on the 2-thiazolylhydrazine scaffold: Synthesis and molecular modeling of selective human monoamine oxidase inhibitors

Franco Chimenti^a, Adriana Bolasco^{a,*}, Daniela Secci^a, Paola Chimenti^a, Arianna Granese^a, Simone Carradori^a, Matilde Yáñez^b, Francisco Orallo^b, Francesco Ortuso^c, Stefano Alcaro^c

^a Dipartimento di Chimica e Tecnologie del Farmaco, Università degli Studi di Roma 'La Sapienza', P.le A. Moro 5, 00185 Rome, Italy

^b Departamento de Farmacología and Instituto de Farmacia Industrial, Facultad de Farmacia, Universidad de Santiago de Compostela, Campus Universitario Sur, E-15782 Santiago de Compostela (La Coruña), Spain

^c Dipartimento di Scienze Farmacobiologiche, Università di Catanzaro 'Magna Graecia', 'Complesso Nini Barbieri', 88021 Roccella di Borgia (CZ), Italy

ARTICLE INFO

Article history:

Received 27 January 2010

Revised 3 June 2010

Accepted 4 June 2010

Available online 9 June 2010

Keywords:

hMAO inhibitors

2-Thiazolylhydrazine

Molecular modeling

ABSTRACT

A new series of [4-(3-methoxyphenyl)-thiazol-2-yl]hydrazine derivatives were synthesized in good yield (71–99%) and characterized by elemental analysis and ¹H NMR studies. The compounds were assayed for their *in vitro* human monoamine oxidase (hMAO) inhibitory activity and selectivity and most of them showed IC₅₀ values in the nanomolar range, thus demonstrating our interest in this privileged scaffold. The most active and selective derivative (**20**), bearing a pyridine moiety on the C=N, displayed IC₅₀ = 3.81 ± 0.12 nM and selectivity ratio = 119 toward hMAO-B. Molecular modeling studies were carried out on recent and high resolution hMAO-A and hMAO-B crystallographic structures to better justify the enzyme–inhibitor interaction toward hMAO isoforms and to explain the structure–activity relationship of this kind of inhibitors.

© 2010 Elsevier Ltd. All rights reserved.

1. Introduction

It is well established that monoamine oxidases (MAOs; EC 1.4.3.4) play a significant role in the control of intracellular concentration of monoaminergic neurotransmitters or neuromodulators such as 5-hydroxytryptamine (5-HT), dopamine (DA), norepinephrine, and dietary amines. The rapid degradation of these molecules ensures the proper functioning of synaptic neurotransmission and is critically important for the regulation of emotional and other brain functions. These flavoenzymes are located predominantly in the outer mitochondrial membrane of neurons, glial, and other mammalian cells. The enzyme exists in two isoforms, MAO-A and -B, sharing about 70% amino acid identity, which are identified by separated encoding genes, tissue distribution, their inhibitor sensitivity and substrate selectivity.¹ Monoamine oxidase-A and -B preferentially deaminate 5-HT and phenylethylamines, respectively. In the case of inhibitor sensitivity, MAO-A and -B forms are inhibited irreversibly by low concentrations of clorgyline and *R*-(-)-deprenyl, respectively. In Figure 1 we collected known clinical MAO inhibitors.

The by-products of MAO-mediated reactions include several chemical species with neurotoxic potential, such as hydrogen peroxide, ammonia (or amine), and aldehydes. It is widely speculated that prolonged or excessive activity of these enzymes may be conducive to mitochondrial damages and neurodegenerative

disturbances. In keeping with these premises, the development of hMAO inhibitors has led to important breakthroughs in the therapy of several neuropsychiatric disorders. Currently, the therapeutic interest in human MAO inhibitors falls into two major categories.² hMAO-A inhibitors are used for the treatment of mental disorders, particularly depression, whereas hMAO-B inhibitors are used as co-adjuvants for the treatment of Parkinson's and Alzheimer's disease. For these reasons, the active site of both isoforms has been recently crystallized with many selective reversible inhibitors to highlight the structural information for the design of new drugs.^{3,4}

After our studies on the pyrazole⁵ and coumarin⁶ derivatives as hMAO inhibitors, we focused our attention on an interesting scaffold of molecules: (4-arylthiazol-2-yl)hydrazines.

In fact, the same development of hMAO inhibitors started with the serendipitous finding of antidepressant effects in patients treated with iproniazid, a hydrazine-based antitubercular agent. An almost common structural feature of substrate and inhibitors usually is an amino or imino group, which seems to play an essential role in orientation and complex formation at the active site of the enzyme. Furthermore, numerous substituted hydrazines have been studied as MAO inhibitors and their specific mechanism of action was fully investigated.⁷ Substituents on the aromatic ring at C4 position of thiazole ring also influenced the activity as demonstrated by the introduction of several groups (NO₂, CN, CH₃, and OCH₃) or halogens (F and Cl) in the *ortho* and *para* positions in our previous works,^{8,9} while the introduction of more steric

* Corresponding author. Tel.: +39 6 49913923; fax: +39 6 4462731.

E-mail address: adriana.bolasco@uniroma1.it (A. Bolasco).

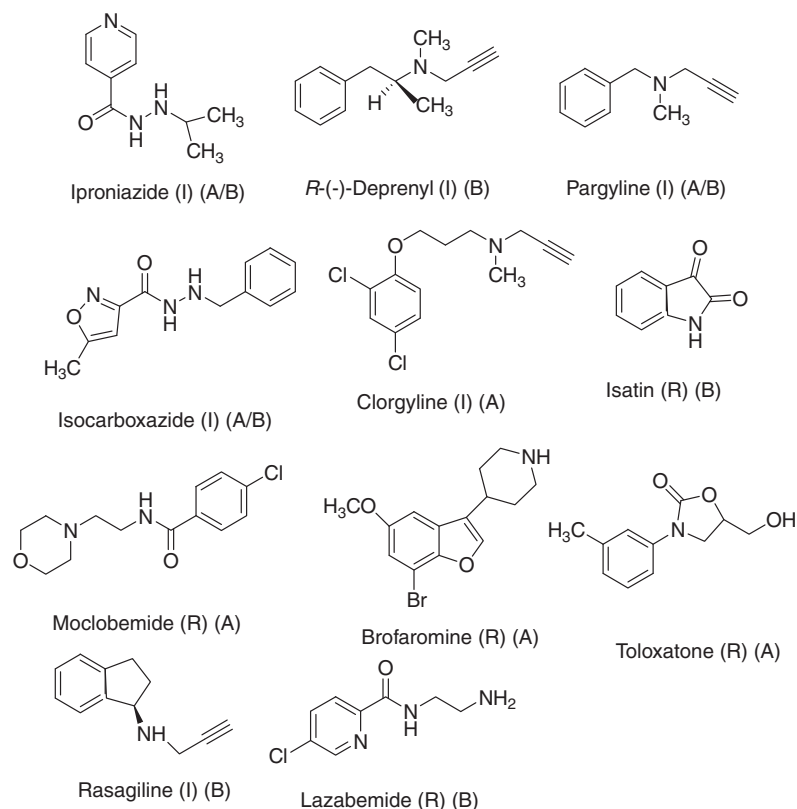


Figure 1. Irreversible (I), reversible (R), and selective hMAO-A (A) and/or hMAO-B (B) inhibitors.

hindered coumarin and naphthalene nucleus at C4 position of thiazole led to a decreased hMAO inhibitory activity.¹⁰ That prompted us to evaluate the presence of an electron-donating group such –OCH₃ in the *meta*-position of the aryl ring. The choice of different aliphatic, cycloaliphatic, heterocyclic, and bicyclic moieties on the C=N group allowed a better comprehension of the steric and electronic influence on the enzyme–inhibitor interaction and a modulation of the chemical structure of these derivatives.

In the past other authors have investigated some hydrazothiazole derivatives as regards their potency as rat MAO inhibitors, and their thermotropic behavior in relation to the partition coefficient in lipid membrane models, correlating a different binding of these inhibitors to the enzyme surface according to their electronic or lipophilic characteristics.¹¹

As our major goal was to obtain a novel lead compound, in this paper we report on the synthesis and the biological activity of a large array of [4-aryl-2-thiazolyl]hydrazines (**1–27**) as hMAO inhibitors, substituted with a methoxy group in the *meta*-position of the aromatic ring, in which the basic function, that supports the primary interaction at the catalytic site, was simulated by the new pharmacophoric structure. Furthermore, we performed a computational study on the most potent inhibitor (**20**) in order to rationalize the enzyme recognition with respect to hMAO-A and hMAO-B. The new, high resolution, Protein Data Bank crystallographic structures were considered as receptor models of hMAO-A (PDB code 2Z5X) and hMAO-B (PDB code 2BK3), respectively.^{3,4}

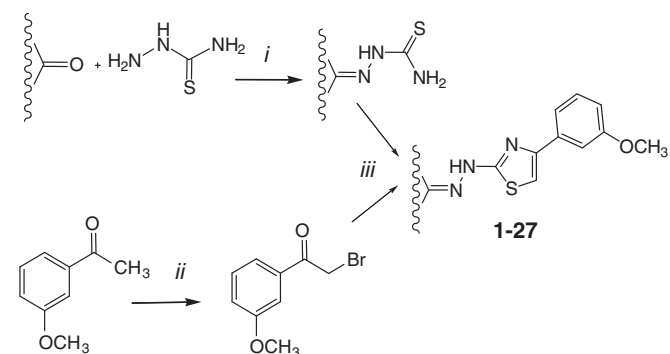
2. Chemistry

[4-Aryl-2-thiazolyl]hydrazine derivatives (**1–27**) were synthesized in high yields (71–99%) as reported in our previous communications^{8–10} (Scheme 1). Different carbonyl compounds reacted directly with thiosemicarbazide in ethanol with catalytic amounts

of acetic acid, and the obtained thiosemicarbazones were subsequently converted into (4-aryl-2-thiazolyl)hydrazines by reaction with α -bromo-3'-methoxyacetophenone in the same solvent (Hantzsch reaction). α -Bromo-3'-methoxyacetophenone has been synthesized by direct halogenation of 3'-methoxyacetophenone with bromine in chloroform. All synthesized products were purified with petroleum ether and diethyl ether and, if requested, by chromatography before characterization by ¹H NMR and elemental analysis (see Section 5 and Supplementary data).

3. Biochemistry

The potential effects of the test drugs on hMAO activity were investigated by measuring their effects on the production of hydrogen peroxide (H₂O₂) from *p*-tyramine (a common substrate for both hMAO-A and hMAO-B), using the Amplex Red MAO assay



Scheme 1. Reagents and conditions: (i) CH₃COOH (cat.), EtOH, rt; (ii) CHCl₃, Br₂, rt; (iii) EtOH, rt.

kit (Molecular Probes, Inc., Eugene, Oregon, USA) and mitochondrial MAO isoforms prepared from insect cells (BTI-TN-5B1-4) infected with recombinant baculovirus containing cDNA inserts for hMAO-A or hMAO-B (Sigma–Aldrich Química S.A., Alcobendas, Spain).

The production of H₂O₂ catalyzed by MAO isoforms can be detected using 10-acetyl-3,7-dihydroxyphenoxazine (Amplex Red reagent), a non-fluorescent and highly sensitive probe that reacts with H₂O₂ in the presence of horseradish peroxidase to produce a fluorescent product, resorufin. In this study, hMAO activity was evaluated using the above method following the general procedure previously described by us.¹² The test drugs (new compounds and reference inhibitors) themselves were unable to react directly with the Amplex Red reagent, which indicates that these drugs do not interfere with the measurements. On the other hand, in our experiments and under our experimental conditions, the control activity of hMAO-A and hMAO-B (using *p*-tyramine as a common substrate for both isoforms) was 165 ± 2 pmol of *p*-tyramine oxidized to *p*-hydroxyphenylacetaldehyde/min ($n = 20$). Most tested drugs concentration-dependently inhibited this enzymatic control activity.

4. Results and discussion

Structure–activity relationships (SARs) were inferred from data of enzymatic experiments reported in Table 1.

With the only exceptions of derivatives **18** and **24**, all tested compounds (assayed as mixture of *E* and *Z* conformers) inhibited hMAOs at micromolar or sub-micromolar concentration with ratio values ranging from <0.0087 (**25**) to 119 (**20**). Aliphatic moieties (**1–5**) showed that hMAO inhibitory activity and selectivity are largely influenced by the chain length. Elongation of the alkyl chain produced slight improvements of hMAO-B inhibition (**1–3**), while the biggest derivatives (**4** and **5**) were endowed with discrete hMAO-A selectivity. Cyclization of the lateral chain of compound **3** to give **6** induced selectivity inversion, but the introduction of a methyl group (**7** and **8**) or further elongation of the aliphatic cycle (**9–13**) improved anti-hMAO-B activity and selectivity (i.e., compound **10**, IC₅₀ hMAO-B = 12.22 ± 0.43 nM and selectivity ratio = 60). It was clearly evident that the anti-hMAO activity and selectivity were strongly associated with the presence of heterocyclic or bicyclic moiety (**13–27**) on the hydrazonic nitrogen. The bulkiest compounds (**23–27**) displayed both low inhibitory activity and the best selectivity toward hMAO-A (compound **25**, IC₅₀ hMAO-A = 874.69 ± 41.43 nM and ratio <0.0087).

Conversely, compounds **14**, **15**, **19**, and **21**, bearing a smaller heterocycle in that position, were quite potent but less selective hMAO-A inhibitors. Great improvement of the hMAO-B inhibitory activity was obtained by replacing the hydrogen atom with a methyl group at the C=N bond (compare compounds **14**, **16**, **19**, and **21–15**, **17**, **20**, and **22**). Among them, compound **20** was the most selective hMAO-B inhibitor and almost five times more potent than *R*(–)-deprenyl (IC₅₀ hMAO-B = 3.81 ± 0.12 nM and selectivity ratio = 119). The presence and the position of a methyl group linked to the pyridine ring deeply affect the hMAO inhibitory activity (**18**, **20**, and **22**) showing the lowest IC₅₀ when it was introduced in the *meta*-position. From the results obtained in this and in our previous works,^{8–10} it is possible to state that moieties on the C4 of the thiazole ring must be carefully evaluated. Molecular modeling studies proved that this region was involved in the interaction between inhibitor and FAD cofactor which was placed inside the active site of the enzyme and was responsible of its oxidative activity. Therefore little changes of substituent dimension in this position were scarcely tolerated. This evidence could be also justified on the basis of the detailed information that PDB provides about the active site of both isoforms: the active site of hMAO-A

is characterized by a single large hydrophobic cavity which adapt itself to the bulkiest moieties better than the two small hydrophobic cavities of hMAO-B. Accordingly, the anti-hMAO activity and selectivity were influenced by the steric hindrance of the substituent on the hydrazonic nitrogen as well. In general, the bulkiest compounds displayed both low inhibitory activity and the best selectivity toward hMAO-A. In the reversibility and irreversibility tests, hMAO-A and hMAO-B inhibition was irreversible in presence of the compound **20**, selected for docking experiments, as shown by the lack enzyme activity restoration after repeated washing. Similar results were obtained for *R*(–)-deprenyl (Table 2). However, significant recovery of hMAO-A and hMAO-B activity was observed after repeated washing of isatin, indicating that this drug is a reversible inhibitor of hMAO isoforms. Similar results were obtained for moclobemide on hMAO-A.

In principle, our results of reversibility with the compound **20** do not seem to correlate well with the conformational analysis made in the docking studies, but a number of arguments may explain, at least in part, this discrepancy. In most cases, the irreversible inhibitors establish a covalent interaction with the active center of the enzyme.¹³ However, not all irreversible inhibitors form covalent adducts with their enzyme targets but they may also act by other mechanisms. In fact, some reversible inhibitors bind so tightly to their target enzyme that they are essentially irreversible. These tight-binding inhibitors may show kinetic properties similar to covalent irreversible inhibitors.

In these cases, some of these inhibitors rapidly bind to the enzyme in a low-affinity enzyme–inhibitor (EI) complex and this then undergoes a slower rearrangement to a very tightly bound EI* complex. This kinetic behavior is called slow-binding. This slow rearrangement after binding often involves a conformational change as the enzyme ‘clamps down’ around the inhibitor molecule.¹⁴ Also some MAO irreversible inhibitors (the so-called suicide inhibitors) act as a substrate for the target enzyme, which finally generates a new compound that irreversibly inhibits MAO activity. Therefore, the initial interaction of these inhibitors with MAO may be different to the interaction obtained after several minutes of the enzyme–inhibitor complex formation. *R*(–)-deprenyl, for example, first of all form a non-covalent complex with MAO as an initial, reversible step. The subsequent interaction of *R*(–)-deprenyl with MAO leads to a reduction of the enzyme-bound flavin adenine dinucleotide, and concomitant oxidation of the inhibitor. This oxidized inhibitor then reacts with FAD at the N5-position in a covalent manner.¹⁵ The initial non-covalent binding to MAO has been also described for other MAO inhibitors.¹⁶ Finally, it is possible that, in some cases of irreversible inhibition, a steric hindrance might not allow the removal of the inhibitor from the enzymatic active center (although its interaction with this binding site is either very weak or reversible).

Bearing in mind all the above considerations and taking into account that the docking studies make only a theoretical prediction of the initial possible interaction inhibitor–enzyme, the results obtained in these docking studies and in the reversibility experiments may be different. Compound **20**, the most potent and selective hMAO-B inhibitor, was submitted to a molecular modeling study with the aim to evaluate its recognition with respect to both A- and B-hMAO isoforms. Two new Protein Data Bank crystal structures were considered, after a preliminary pre-treatment, as receptor models of hMAO-A and hMAO-B (see Section 5). The ligand was built taking into account both *E* and *Z* isomers and submitted to Monte Carlo conformational search followed by Boltzmann population analysis at 300 K. Such an investigation revealed the much higher probability of existence for *E* isomer (99.6%) with respect to the *Z* one (0.4%) but, in order to analyze the binding modes of **20**, we decided to consider both global minimum energy structures for the next docking simulations. These calculations were

Table 1
Structures and biological activity of derivatives **1–27** and reference inhibitors

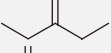
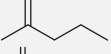
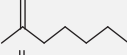
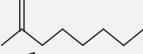
Compound	X	IC ₅₀ hMAO-A	IC ₅₀ hMAO-B	Ratio
1		4.43 ± 0.22 μM	5.07 ± 0.13 μM	0.87
2		824.33 ± 40.05 nM	771.82 ± 30.05 nM	1.1
3		1.31 ± 0.03 μM ^b	871.47 ± 38.61 nM	1.5
4		1.15 ± 0.01 μM ^a	6.72 ± 0.32 μM	0.17
5		1.38 ± 0.04 μM	***	< 0.014 [#]
6		591.80 ± 23.13 nM ^b	1.06 ± 0.07 μM	0.56
7		836.21 ± 36.58 nM ^a	26.64 ± 0.81 nM	31
8		1.45 ± 0.04 μM ^a	231.02 ± 9.61 nM	6.3
9		1.91 ± 0.04 μM ^a	31.87 ± 1.26 nM	60
10		737.40 ± 21.42 nM ^a	12.22 ± 0.43 nM	60
11		678.75 ± 32.15 nM ^a	72.70 ± 2.31 nM	9.3
12		749.15 ± 31.62 nM ^a	35.49 ± 1.27 nM	21
13		1.78 ± 0.05 μM ^a	29.54 ± 1.07 nM	60
14		342.88 ± 15.62 nM ^a	6.78 ± 0.25 μM	0.051
15		333.05 ± 16.08 nM ^b	1.68 ± 0.06 μM	0.20
16		457.73 ± 20.35 nM	493.83 ± 16.30 nM	0.93
17		636.08 ± 27.65 nM	551.38 ± 12.35 nM	1.15
18		***	***	
19		537.66 ± 27.35 nM ^b	2.91 ± 0.13 μM	0.18
20		455.16 ± 20.43 nM ^a	3.81 ± 0.12 nM	119
21		697.53 ± 19.73 nM ^b	1.14 ± 0.03 μM	0.61
22		3.71 ± 0.08 μM ^a	116.38 ± 4.25 nM	32
23		3.64 ± 0.06 μM	***	<0.036 [#]

Table 1 (continued)

Compound	X	IC ₅₀ hMAO-A	IC ₅₀ hMAO-B	Ratio
24		***	**	
25		874.69 ± 41.43 nM	***	<0.0087 [#]
26		413.81 ± 21.17 nM ^b	799.69 ± 27.61 nM	0.52
27		5.56 ± 0.17 μM	6.97 ± 0.23 μM	0.80
C		4.46 ± 0.22 nM ^a	61.35 ± 1.13 μM	0.000073
D		67.25 ± 1.02 μM	19.60 ± 0.86 nM	3431
I		6.56 ± 0.26 μM	7.54 ± 0.36 μM	0.87
M		361.38 ± 19.37 μM	*	<0.36 [§]
Is		***	18.75 ± 1.24 μM	>5.3 [£]

C, clorgyline; D, *R*-(–)-deprenyl; I, iproniazid; M, moclobemide; Is, isatin. Ratio: hMAO-B selectivity index = IC₅₀(hMAO-A)/IC₅₀(hMAO-B). Each IC₅₀ value is the mean ± SEM from five experiments. Level of statistical significance: ^a*P* < 0.01 or ^b*P* < 0.05 versus the corresponding IC₅₀ values obtained against hMAO-B, as determined by ANOVA/Dunnett's.

* Inactive at 1 mM (highest concentration tested).

** Inactive at 100 μM (highest concentration tested).

*** One hundred micromolar inhibits the corresponding hMAO activity by approximately 40–45%. At higher concentration the compounds precipitate.

[#] Values obtained under the assumption that the corresponding IC₅₀ against hMAO-B is the highest concentration tested (100 μM).

[§] Value obtained under the assumption that the corresponding IC₅₀ against hMAO-B is the highest concentration tested (1 mM).

[£] Value obtained under the assumption that the corresponding IC₅₀ against hMAO-A is the highest concentration tested (100 μM).

Table 2

Reversibility and irreversibility of hMAO inhibition of derivative **20** and reference inhibitors

Compound	% hMAO-A inhibition		% hMAO-B inhibition	
	Before washing	After repeated washing	Before washing	After repeated washing
<i>R</i> -(–)-Deprenyl (20 nM)				
Moclobemide (500 μM)	86.75 ± 4.34	10.26 ± 0.65 ^a	51.45 ± 2.16	52.05 ± 2.08
Isatin (100 μM)	40.32 ± 1.83	12.10 ± 0.52 ^a		
Isatin (50 μM)			84.36 ± 3.24	16.62 ± 0.71 ^a
20 (500 nM)	59.14 ± 2.02	65.13 ± 2.94		
20 (5 nM)			63.73 ± 3.12	67.18 ± 3.21

Each value is the mean ± SEM from five experiments (*n* = 5).

^a Level of statistical significance: *P* < 0.01 versus the corresponding % hMAO-A or hMAO-B inhibition before washing, as determined by ANOVA/Dunnett's.

performed onto hMAO-A and hMAO-B receptor models and the recognition of **20** was evaluated using the interaction energy parameter (Table 3).

As reported in Table 3, in agreement with the experimental data, compound **20** highlighted a better interaction to hMAO-B than hMAO-A. The interaction energy components analysis indicated a complete preference of compound **20** with respect to the B isoform in terms of both vdW and electrostatic contributions. These results were submitted to graphical inspection and the most stable configurations of **20** in both enzymes were displayed in Figure 2. The analysis of compound **20** binding modes revealed that the *E* isomer was more favoured than the *Z* on both receptor models. The configuration of compound **20** in hMAO-A and hMAO-B was similar showing, in both case, the *m*-methoxyphenyl moiety directed toward the FAD cofactor and the pyridine ring toward the catalytic cleft outer side. Even if the number of interacting residues was slightly larger with hMAO-A, the hMAO-B recognition reported much more productive contributions: the ligand showed a deeper position that allowed it to perform stacking contacts to

Table 3

Interaction energies (kcal/mol) of compound **20** within hMAO-A and hMAO-B binding pockets

	Δ <i>E</i> _{int}	vdW	EI
hMAO-A	–2.70	–7.20	4.50
hMAO-B	–36.70	–36.30	–0.40

Δ*E*_{int}, total interaction energy; vdW, van der Waals contribution; EI, electrostatic contribution.

Tyr398 and one hydrogen bond was established to the Ile198 backbone.

Moreover, into the preferred isoform, the *m*-methoxyphenyl group was located close to Tyr188, Phe343, and Tyr435 and the pyridine moiety was less exposed toward the solvent than into the hMAO-A. The graphical inspection allowed a better appreciation of the details of the isoform recognition taking into account the known differences in the binding pockets of MAO-A and -B. In particular the corresponding residues Ile335 (hMAO-A) and

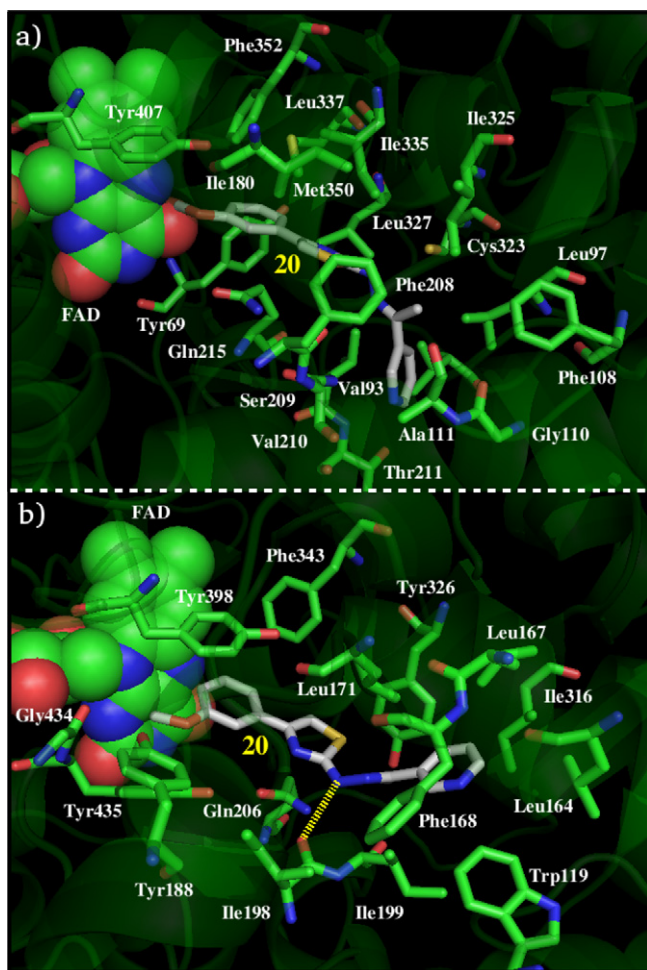


Figure 2. Compound **20** recognition of hMAO-A (a) and hMAO-B (b). Ligand is reported in sticks, interacting residues in green carbon colored sticks, FAD cofactor is displayed as a spacefill structure. The rest of the enzyme is displayed in transparent green cartoon. Yellow dotted line indicates hydrogen bond interaction.

Tyr326 (hMAO-B) appeared relevant to explain the molecular recognition of the compound **20**. In the B isoform Tyr326, due to its consistent steric effects, induced the inhibitor to interact with the FAD. Conversely, the hMAO-A Ile335, characterized by a lower hindrance with respect to the corresponding hMAO-B residue, allowed the ligand to assume multiple poses into the binding cleft with higher enthalpic and entropic penalties.

We found a molecular rationale for the hMAO-A and hMAO-B selectivity of this new class of 2-thiazolylhydrazine inhibitors. These findings increase our confidence in our model and stimulate us to continue our investigations in designing more potent and selective analogs. The results obtained in this study indicate that some of the compounds tested may have interesting therapeutic potential as original chemical models (templates) for the design and subsequent development of new drugs (potent and selective hMAO-A or hMAO-B inhibitors) useful for improving the pharmacological treatment of major depressive disorders and neurodegenerative diseases (e.g., Parkinson's disease), respectively.

5. Experimental

5.1. Chemistry

Starting materials and reagents were obtained from commercial suppliers and were used without purification. Melting points (mp)

were determined by the capillary method on an FP62 apparatus (Mettler-Toledo) and are uncorrected. ^1H NMR spectra were recorded at 400 MHz on a Bruker spectrometer using $\text{DMSO}-d_6$ or CDCl_3 as solvent. Chemical shifts are expressed as δ units (ppm) relative to TMS. Coupling constants J are expressed in hertz (Hz). Elemental analyses for C, H, and N were determined with a Perkin-Elmer 240 B microanalyzer and the analytical results were $\geq 95\%$ purity for all compounds. All reactions were monitored by TLC performed on 0.2 mm thick silica gel plates (60 F₂₅₄ Merck). Preparative flash column chromatography was carried out on silica gel (230–400 mesh, G60 Merck). Organic solutions were dried over anhydrous sodium sulfate. Concentration and evaporation of the solvent after reaction or extraction was carried out on a rotary evaporator (Büchi Rotavapor) operating at reduced pressure. Compound **17** is also commercially available.

5.2. General procedure for the synthesis of α -bromo-3'-methoxyacetophenone

Equimolar quantities of 3'-methoxyacetophenone and bromine, both dissolved in chloroform, were stirred for 4 h at room temperature until the presence of HBr disappeared. The solution was evaporated under vacuum and the pale yellow solid was washed with petroleum ether to give the product in good yield (97%).

5.3. General procedure for the synthesis of derivatives 1–27

The appropriate carbonyl compound (50 mmol) was dissolved in 100 mL of ethanol and stirred with an equimolar quantity of thiosemicarbazide for 24 h at room temperature with catalytic amounts of acetic acid. The desired thiosemicarbazone precipitated from reaction mixture was filtered, washed with suitable solvent (petroleum ether, hexane, and diethyl ether), and dried. Equimolar amounts of the prepared thiosemicarbazone (50 mmol) and freshly synthesized α -bromo-3'-methoxyacetophenone (50 mmol) were reacted in ethanol at room temperature under magnetic stirring for 4 h. The suspension was filtered and dried to give compounds **1–27** in high yield.

5.3.1. 1-(4-(3-Methoxyphenyl)thiazol-2-yl)-2-(propan-2-ylidene)hydrazine (**1**)

Yield 99%; mp 213–214 °C; ^1H NMR (CDCl_3) 2.12 (s, 3H, CH_3), 2.21 (s, 3H, CH_3), 3.90 (s, 3H, OCH_3), 6.70 (s, 1H, C_5H -thiaz.), 6.98–7.01 (m, 1H, Ar), 7.26–7.29 (m, 2H, Ar), 7.37–7.39 (m, 1H, Ar), 12.45 (br s, 1H, NH, D_2O exch.).

5.3.2. 1-(4-(3-Methoxyphenyl)thiazol-2-yl)-2-(pentan-3-ylidene)hydrazine (**2**)

Yield 89%; mp 158–159 °C; ^1H NMR (CDCl_3) 1.14–1.18 (m, 3H, CH_3), 1.23–1.27 (m, 3H, CH_3), 2.41–2.43 (m, 2H, CH_2), 2.55–2.57 (m, 2H, CH_2), 3.91 (s, 3H, OCH_3), 6.69 (s, 1H, C_5H -thiaz.), 7.01 (s, 1H, Ar), 7.27–7.28 (m, 2H, Ar), 7.37–7.39 (m, 1H, Ar), 12.35 (br s, 1H, NH, D_2O exch.).

5.3.3. 1-(4-(3-Methoxyphenyl)thiazol-2-yl)-2-(pentan-2-ylidene)hydrazine (**3**)

Yield 84%; mp 150–151 °C; ^1H NMR (CDCl_3) 0.96–1.00 (m, 3H, CH_3), 1.65–1.68 (m, 2H, CH_2), 2.15 (s, 3H, CH_3), 2.36–2.38 (m, 2H, CH_2), 3.93 (s, 3H, OCH_3), 6.70 (s, 1H, C_5H -thiaz.), 6.98–7.00 (m, 1H, Ar), 7.37–7.40 (m, 3H, Ar), 12.29 (br s, 1H, NH, D_2O exch.).

5.3.4. 1-(4-(3-Methoxyphenyl)thiazol-2-yl)-2-(heptan-2-ylidene)hydrazine (**4**)

Yield 89%; mp 134–135 °C; ^1H NMR (CDCl_3) 0.90–0.93 (m, 3H, CH_3), 1.34–1.35 (m, 2H, CH_2), 1.56–1.63 (m, 4H, $2 \times \text{CH}_2$), 2.19 (s, 3H, CH_3), 2.35–2.39 (m, 2H, CH_2), 3.93 (s, 3H, OCH_3), 6.69

(s, 1H, C₅H-thiaz.), 7.01 (s, 1H, Ar), 7.27–7.30 (m, 2H, Ar), 7.37–7.39 (m, 1H, Ar), 12.30 (br s, 1H, NH, D₂O exch.).

5.3.5. 1-(4-(3-Methoxyphenyl)thiazol-2-yl)-2-(octan-2-ylidene)hydrazine (5)

Yield 99%; mp 109–110 °C; ¹H NMR (DMSO-*d*₆) 0.86 (s, 3H, CH₃), 1.27–2.49 (m, 10H, CH₂), 2.49 (s, 3H, CH₃), 3.78 (s, 3H, OCH₃), 6.65 (s, 1H, C₅H-thiaz.), 6.96–6.99 (m, 2H, Ar), 7.09 (s, 1H, Ar), 7.72–7.75 (m, 2H, Ar), 11.20 (br s, 1H, NH, D₂O exch.).

5.3.6. 1-(4-(3-Methoxyphenyl)thiazol-2-yl)-2-cyclopentylidenehydrazine (6)

Yield 73%; mp 185–186 °C; ¹H NMR (CDCl₃) 1.85–1.87 (m, 2H, cyclopentyl), 1.93–1.97 (m, 2H, cyclopentyl), 2.53–2.55 (m, 2H, cyclopentyl), 2.65–2.67 (m, 2H, cyclopentyl), 3.91 (s, 3H, OCH₃), 6.62 (s, 1H, C₅H-thiaz.), 7.00 (m, 1H, Ar), 7.26–7.29 (m, 2H, Ar), 7.30–7.38 (m, 1H, Ar), 12.28 (br s, 1H, NH, D₂O exch.).

5.3.7. 1-(4-(3-Methoxyphenyl)thiazol-2-yl)-2-(2-methylcyclopentylidene)hydrazine (7)

Yield 79%; mp 172–173 °C; ¹H NMR (CDCl₃) 1.20 (s, 3H, CH₃), 1.21 (s, 1H, cyclopentyl), 1.60–1.61 (m, 2H, cyclopentyl), 2.75–2.90 (m, 2H, cyclopentyl), 3.92 (s, 3H, OCH₃), 6.72 (s, 1H, C₅H-thiaz.), 7.00 (s, 1H, Ar), 7.26–7.29 (m, 2H, Ar), 7.30–7.38 (m, 1H, Ar), 12.28 (br s, 1H, NH, D₂O exch.).

5.3.8. 1-(4-(3-Methoxyphenyl)thiazol-2-yl)-2-(3-methylcyclopentylidene)hydrazine (8)

Yield 99%; mp 189–190 °C; ¹H NMR (DMSO-*d*₆) 1.00–1.03 (m, 3H, CH₃), 1.12–1.15 (m, 1H, cyclopentyl), 1.89–2.43 (m, 5H, cyclopentyl), 2.5–2.67 (m, 1H, cyclopentyl), 3.90 (s, 3H, OCH₃), 6.61 (s, 1H, C₅H-thiaz.), 7.24–7.38 (m, 4H, Ar), 10.70 (br s, 1H, NH, D₂O exch.).

5.3.9. 1-(4-(3-Methoxyphenyl)thiazol-2-yl)-2-cyclohexylidenehydrazine (9)

Yield 76%; mp 181–182 °C; ¹H NMR (CDCl₃) 1.57–1.60 (m, 4H, cyclohexyl), 1.62–1.66 (m, 2H, cyclohexyl), 1.68–1.79 (m, 2H, cyclohexyl), 2.66–2.72 (m, 2H, cyclohexyl), 3.91 (s, 3H, OCH₃), 6.69 (s, 1H, C₅H-thiaz.), 7.00–7.01 (m, 1H, Ar), 7.26–7.29 (m, 1H, Ar), 7.30–7.39 (m, 2H, Ar), 12.28 (br s, 1H, NH, D₂O exch.).

5.3.10. 1-(4-(3-Methoxyphenyl)thiazol-2-yl)-2-(2-methylcyclohexylidene)hydrazine (10)

Yield 99%; mp 156–157 °C; ¹H NMR (CDCl₃) 1.15–1.16 (m, 3H, CH₃), 1.58–1.59 (m, 2H, cyclohexyl), 1.60–1.62 (m, 1H, cyclohexyl), 1.80–1.90 (m, 1H, cyclohexyl), 2.00–2.07 (m, 2H, cyclohexyl), 2.19–2.89 (m, 3H, cyclohexyl), 3.91 (s, 3H, OCH₃), 6.60 (s, 1H, C₅H-thiaz.), 7.00 (s, 1H, Ar), 7.26–7.29 (m, 2H, Ar), 7.30–7.38 (m, 1H, Ar), 12.20 (br s, 1H, NH, D₂O exch.).

5.3.11. 1-(4-(3-Methoxyphenyl)thiazol-2-yl)-2-(3-methylcyclohexylidene)hydrazine (11)

Yield 93%; mp 148–149 °C; ¹H NMR (CDCl₃) 1.02–1.03 (m, 3H, CH₃), 1.09–1.11 (m, 2H, cyclohexyl), 1.58–1.69 (m, 5H, cyclohexyl), 2.38–2.40 (m, 1H, cyclohexyl), 3.18–3.20 (m, 1H, cyclohexyl), 3.91 (s, 3H, OCH₃), 6.67 (s, 1H, C₅H-thiaz.), 7.01 (s, 1H, Ar), 7.22–7.28 (m, 2H, Ar), 7.30–7.36 (m, 1H, Ar), 12.18 (br s, 1H, NH, D₂O exch.).

5.3.12. 1-(4-(3-Methoxyphenyl)thiazol-2-yl)-2-(4-methylcyclohexylidene)hydrazine (12)

Yield 76%; mp 152–153 °C; ¹H NMR (CDCl₃) 0.98 (s, 3H, CH₃), 1.24–1.25 (m, 2H, cyclohexyl), 1.34–1.45 (m, 2H, cyclohexyl), 1.57–1.66 (m, 2H, cyclohexyl), 1.90–2.01 (m, 1H, cyclohexyl), 2.20–3.20 (m, 2H, cyclohexyl), 3.92 (s, 3H, OCH₃), 6.67 (s, 1H,

C₅H-thiaz.), 7.01 (s, 1H, Ar), 7.26–7.29 (m, 2H, Ar), 7.30–7.41 (m, 1H, Ar), 12.24 (br s, 1H, NH, D₂O exch.).

5.3.13. 1-(4-(3-Methoxyphenyl)thiazol-2-yl)-2-cycloheptylidenehydrazine (13)

Yield 71%; mp 194–195 °C; ¹H NMR (CDCl₃) 1.57–1.60 (m, 4H, cycloheptyl), 1.65–1.67 (m, 4H, cycloheptyl), 2.80–2.86 (m, 2H, cycloheptyl), 2.87–2.90 (m, 2H, cycloheptyl), 3.92 (s, 3H, OCH₃), 7.26 (s, 1H, C₅H-thiaz.), 7.27–7.29 (m, 1H, Ar), 7.30–7.33 (m, 3H, Ar), 12.30 (br s, 1H, NH, D₂O exch.).

5.3.14. 1-(4-(3-Methoxyphenyl)thiazol-2-yl)-2-(furan-2-ylmethylene)hydrazine (14)

Yield 99%; mp 139–140 °C; ¹H NMR (DMSO-*d*₆) 3.98 (s, 3H, OCH₃), 7.72–7.91 (m, 3H, furan), 7.90 (s, 1H, C₅H-thiaz.), 8.33–8.72 (m, 4H, Ar), 9.08 (s, 1H, CH=), 11.95 (br s, 1H, NH, D₂O exch.).

5.3.15. 1-(4-(3-Methoxyphenyl)thiazol-2-yl)-2-(1-(furan-2-yl)ethylidene)hydrazine (15)

Yield 80%; mp 224–225 °C; ¹H NMR (DMSO-*d*₆) 2.23 (s, 3H, CH₃), 3.78 (s, 3H, OCH₃), 6.60 (s, 1H, C₅H-thiaz.), 6.75–6.98 (m, 2H, furan), 7.33–7.42 (m, 4H, Ar), 7.58 (s, 1H, furan), 11.28 (br s, 1H, NH, D₂O exch.).

5.3.16. 1-(4-(3-Methoxyphenyl)thiazol-2-yl)-2-(thiophen-2-ylmethylene)hydrazine (16)

Yield 82%; mp 185–186 °C; ¹H NMR (DMSO-*d*₆) 3.78 (s, 3H, OCH₃), 6.80 (s, 1H, C₅H-thiaz.), 7.08–7.10 (m, 1H, thiophene), 7.30–7.32 (m, 1H, thiophene), 7.33–7.40 (m, 4H, Ar), 7.56–7.58 (m, 1H, thiophene), 8.22 (s, 1H, CH=), 12.22 (br s, 1H, NH, D₂O exch.).

5.3.17. 1-(4-(3-Methoxyphenyl)thiazol-2-yl)-2-(1-(thiophen-2-yl)ethylidene)hydrazine (17)

Yield 75%; mp 220–221 °C; ¹H NMR (DMSO-*d*₆) 2.33 (s, 3H, CH₃), 3.79 (s, 3H, OCH₃), 6.80 (s, 1H, C₅H-thiaz.), 7.05–7.07 (m, 1H, thiophene), 7.30–7.38 (m, 2H, thiophene), 7.42–7.52 (m, 4H, Ar), 11.40 (br s, 1H, NH, D₂O exch.).

5.3.18. 1-(4-(3-Methoxyphenyl)thiazol-2-yl)-2-(1-(pyridin-2-yl)ethylidene)hydrazine (18)

Yield 75%; mp 236–237 °C; ¹H NMR (DMSO-*d*₆) 2.45 (s, 3H, CH₃), 3.79 (s, 3H, OCH₃), 7.90 (s, 1H, C₅H-thiaz.), 8.28–8.35 (m, 4H, Ar), 8.40–8.78 (m, 4H, pyridine), 10.90 (br s, 1H, NH, D₂O exch.).

5.3.19. 1-(4-(3-Methoxyphenyl)thiazol-2-yl)-2-(pyridin-3-ylmethylene)hydrazine (19)

Yield 99%; mp 214–215 °C; ¹H NMR (DMSO-*d*₆) 3.80 (s, 3H, OCH₃), 6.88 (s, 1H, C₅H-thiaz.), 7.31–7.35 (m, 1H, Ar), 7.41–7.45 (m, 3H, Ar), 8.14–8.15 (m, 1H, pyridine), 8.62–8.70 (m, 3H, pyridine), 9.03 (s, 1H, CH=), 12.30 (br s, 1H, NH, D₂O exch.).

5.3.20. 1-(4-(3-Methoxyphenyl)thiazol-2-yl)-2-(1-(pyridin-3-yl)ethylidene)hydrazine (20)

Yield 89%; mp 249–250 °C; ¹H NMR (DMSO-*d*₆) 2.40 (s, 3H, CH₃), 3.79 (s, 3H, OCH₃), 6.89 (s, 1H, C₅H-thiaz.), 7.33–7.35 (m, 1H, Ar), 7.44–7.51 (m, 3H, Ar), 8.19–8.20 (m, 2H, pyridine), 8.83–8.85 (m, 2H, pyridine), 12.25 (br s, 1H, NH, D₂O exch.).

5.3.21. 1-(4-(3-Methoxyphenyl)thiazol-2-yl)-2-(pyridin-4-ylmethylene)hydrazine (21)

Yield 99%; mp 250–251 °C; ¹H NMR (DMSO-*d*₆) 3.79 (s, 3H, OCH₃), 6.88 (s, 1H, C₅H-thiaz.), 7.37–7.45 (m, 3H, Ar), 7.55 (s, 1H, Ar), 8.10–8.13 (m, 4H, pyridine), 8.81 (s, 2H, CH=), 13.10 (br s, 1H, NH, D₂O exch.).

5.3.22. 1-(4-(3-Methoxyphenyl)thiazol-2-yl)-2-(1-(pyridin-4-yl)ethylidene)hydrazine (22)

Yield 80%; mp 169–170 °C; ¹H NMR (DMSO-*d*₆) 2.40 (s, 3H, CH₃), 3.79 (s, 3H, OCH₃), 6.81 (s, 1H, C₅H-thiaz.), 7.33–7.35 (m, 1H, Ar), 7.40–7.45 (m, 3H, Ar), 8.15–8.16 (m, 2H, pyridine), 8.81–8.83 (m, 2H, pyridine), 12.20 (br s, 1H, NH, D₂O exch.).

5.3.23. 1-(4-(3-Methoxyphenyl)thiazol-2-yl)-2-(naphthalen-1-ylmethylene)hydrazine (23)

Yield 85%; mp 201–202 °C; ¹H NMR (DMSO-*d*₆) 3.80 (s, 3H, OCH₃), 6.92 (s, 1H, C₅H-thiaz.), 7.38–7.46 (m, 3H, Ar), 7.59–7.67 (m, 3H, Ar), 7.96–7.99 (m, 3H, Ar), 8.25–8.30 (m, 2H, Ar), 8.91 (s, 1H, CH=), 11.45 (br s, 1H, NH, D₂O exch.).

5.3.24. 1-(4-(3-Methoxyphenyl)thiazol-2-yl)-2-(1-(naphthalen-2-yl)ethylidene)hydrazine (24)

Yield 77%; mp 235–236 °C; ¹H NMR (DMSO-*d*₆) 2.42 (s, 3H, CH₃), 3.79 (s, 3H, OCH₃), 6.95 (s, 1H, C₅H-thiaz.), 7.25–7.48 (m, 7H, Ar), 7.90–8.20 (m, 4H, Ar), 11.30 (br s, 1H, NH, D₂O exch.).

5.3.25. 1-(4-(3-Methoxyphenyl)thiazol-2-yl)-2-(benzodioxol-5-ylmethylene)-hydrazine (25)

Yield 79%; mp 229–230 °C; ¹H NMR (DMSO-*d*₆) 3.62 (s, 3H, OCH₃), 6.06 (s, 2H, OCH₂O), 6.84 (s, 1H, C₅H-thiaz.), 7.01–7.40 (m, 7H, Ar), 7.99 (s, 1H, CH=), 12.19 (br s, 1H, NH, D₂O exch.).

5.3.26. 1-(4-(3-Methoxyphenyl)thiazol-2-yl)-2-((1H-indol-3-yl)methylene)-hydrazine (26)

Yield 75%; mp 229–230 °C; ¹H NMR (DMSO-*d*₆) 3.79 (s, 3H, OCH₃), 6.96 (s, 1H, C₅H-thiaz.), 7.15–7.23 (m, 4H, Ar), 7.30–7.44 (m, 4H, indole), 7.77 (s, 1H, CH=), 8.23 (s, 1H, NH-indole, D₂O exch.), 11.55 (br s, 1H, NH, D₂O exch.).

5.3.27. 1-(4-(3-Methoxyphenyl)thiazol-2-yl)-2-(1-(coumarin-3-yl)ethylidene)hydrazine (27)

Yield 95%; mp 242–243 °C; ¹H NMR (DMSO-*d*₆) 2.27 (s, 3H, CH₃), 3.79 (s, 3H, OCH₃), 6.90 (s, 1H, C₅H-thiaz.), 7.37–7.40 (m, 4H, Ar), 7.44–7.45 (m, 2H, coumarin), 7.50–7.70 (m, 2H, coumarin), 8.16 (s, 1H, ArCH=), 11.40 (br s, 1H, NH, D₂O exch.).

5.4. Determination of hMAO isoform activity

The effects of the test compounds on the enzymatic activity of hMAO isoform were evaluated by a fluorimetric method following the experimental protocol previously described by us.¹² Briefly, 0.1 mL of sodium phosphate buffer (0.05 M, pH 7.4) containing different concentrations of the test drugs (new compounds or reference inhibitors) and adequate amounts of recombinant hMAO-A or hMAO-B required and adjusted to obtain in our experimental conditions the same reaction velocity, that is, to oxidize (in the control group) 165 pmol of *p*-tyramine/min (hMAO-A: 1.1 μg protein; specific activity: 150 nmol of *p*-tyramine oxidized to *p*-hydroxyphenylacetaldehyde/min/mg protein; hMAO-B: 7.5 μg protein; specific activity: 22 nmol of *p*-tyramine transformed/min/mg protein) were incubated for 15 min at 37 °C in a flat-black-bottomed 96-well microtest plate (BD Biosciences, Franklin Lakes, NJ, USA) placed in the dark multimode microplate reader chamber. After this incubation period, the reaction was started by adding (final concentrations) 200 μM Amplex Red reagent, 1 U/mL horseradish peroxidase, and 1 mM *p*-tyramine (final saturating concentration). The production of H₂O₂ and, consequently, of resorufin was quantified at 37 °C in a multidetection microplate fluorescence reader (Fluostar Optima, BMG Labtech GmbH, Offenburg, Germany) based on the fluorescence generated (excitation, 545 nm, emission, 590 nm) over a 15 min period, in which the fluorescence increased linearly. Control experiments were carried out

simultaneously by replacing the test drugs (new compounds and reference inhibitors) with appropriate dilutions of the vehicles. In addition, the possible capacity of the above test drugs to modify the fluorescence generated in the reaction mixture due to non-enzymatic inhibition (e.g., for directly reacting with Amplex Red reagent) was determined by adding these drugs to solutions containing only the Amplex Red reagent in a sodium phosphate buffer.

The specific fluorescence emission (used to obtain the final results) was calculated after subtraction of the background activity, which was determined from vials containing all components except the hMAO isoforms, which were replaced by a sodium phosphate buffer solution. In our experimental conditions, this background activity was practically negligible.

5.5. Reversibility and irreversibility experiments

To evaluate whether the compound **20** is reversible or irreversible hMAO inhibitor, an effective centrifugation–ultrafiltration method (so-called repeated washing) previously described by us was used.⁷ Briefly, adequate amounts of recombinant hMAO-A or hMAO-B were incubated together with a single concentration (see Table 2) of the compound **20** or the reference inhibitors *R*(–)-deprenyl, isatin, and moclobemide in a sodium phosphate buffer (0.05 M, pH 7.4) for 15 min at 37 °C. After this incubation period, an aliquot of this sample was stored at 4 °C and used for subsequent measurement of hMAO activity under the experimental conditions indicated above (see the Section 5.4). The remaining incubated sample (300 μL) was placed in an Ultrafree-0.5 centrifugal tube (Millipore, Billerica, USA) with a 30 kDa Biomax membrane in the middle of the tube and centrifuged (9000g, 20 min, 4 °C) in a centrifuge (J2-MI, Beckman Instruments, Inc., Palo Alto, California, USA). The enzyme retained in the 30 kDa membrane was resuspended in sodium phosphate buffer at 4 °C and centrifuged again (under the same experimental conditions described above) two successive times. After the third centrifugation, the enzyme retained in the membrane was resuspended in sodium phosphate buffer (300 μL) and an aliquot of this suspension was used for subsequent hMAO isoform activity determination. Control experiments were performed simultaneously (to define 100% hMAO activity) by replacing the test drugs with appropriate dilutions of the vehicles. The corresponding values of percent (%) hMAO isoform inhibition were separately calculated for samples with and without repeated washing. Furthermore, *K*_i values for each compound have been calculated and reported in Supplementary data.

5.6. Molecular modeling

The Protein Data Bank¹⁷ (PDB) crystallographic structures 2Z5X³ and 2BK3⁴ were considered as receptor models of hMAO-A and hMAO-B, respectively. Both *E* and *Z* isomers of compound **20** were built by means of the Maestro GUI.¹⁸ 2000 steps of Monte Carlo conformational search were applied to all rotatable bonds of this inhibitor. The OPLS-AA¹⁹ force field, as implemented in the version 7.2 of MacroModel software,²⁰ was adopted to evaluate the energy of the Monte Carlo structures. Water solvent effects were taken into account using the implicit solvation model GB/SA.²¹ Such an approach led to the identification of 66 and 72 unique conformations for the *E* and *Z* isomers, respectively. The Boltzmann analysis was applied to both Monte Carlo structure ensembles reporting a *E*:*Z* population ratio equal to 99.6:0.4. The global minimum energy structures of *E* and *Z* isomers were submitted to docking simulations with respect to hMAO-A and -B PDB crystallographic structures. Both receptor models required graphical manipulation: the co-crystallized ligands, harmine and farnesol, respectively, for 2Z5X and 2BK3, were removed, FAD

double bonds were fixed, and hydrogen atoms were added onto both proteins and cofactors. According to the Glide²² methodology, a regular box, of about 110,000 Å³, centered onto the cofactor N5 atom, was considered as the enzyme active site for both hMAO-A and -B models. In order to take into account the induced fit phenomena, the ligand was docked using the Glide 'flexible' algorithm. The binding affinity was evaluated using the free energy of complexation (Ecvdw). The most stable complexes were submitted to energy minimization using the same force field and aqueous environment previously reported. The resulting optimized structures were considered for the binding modes graphical analysis. PyMol ver. 0.98²³ was used to create Figure 2.

Acknowledgments

This work was supported by grants from MURST (Italy). Ministerio de Sanidad y Consumo (Spain; FISS PI061537) and Consellería de Innovación e Industria de la Xunta de Galicia (Spain; INCI-TE07PXI203039ES, INCITE08E1R203054ES, and 08CSA019203PR).

Supplementary data

Supplementary data associated with this article can be found, in the online version, at doi:10.1016/j.bmc.2010.06.007.

References and notes

- Edmondson, D. E.; Binda, C.; Wang, J.; Upadhyay, A. K.; Mattevi, A. *Biochemistry* **2009**, *48*, 4220.
- (a) Youdim, M. B. H.; Edmondson, D.; Tipton, K. F. *Nat. Rev. Neurosci.* **2006**, *7*, 295; (b) Bortolato, M.; Chen, K.; Shih, J. C. *Adv. Drug Delivery Rev.* **2008**, *60*, 1527.
- Son, S. Y.; Ma, J.; Kondou, Y.; Yoshimura, M.; Yamashita, E.; Tsukihara, T. *Proc. Natl. Acad. Sci. U.S.A.* **2008**, *105*, 5739. Data deposition: www.pdb.org (PDB ID code 2Z5X).
- Hubálek, F.; Binda, C.; Khalil, A.; Li, M.; Mattevi, A.; Castagnoli, N.; Edmondson, D. E. *J. Biol. Chem.* **2005**, *280*, 15761. Data deposition: www.pdb.org (PDB ID code 2BK3).
- (a) Chimenti, F.; Maccioni, E.; Secci, D.; Bolasco, A.; Chimenti, P.; Granese, A.; Befani, O.; Turini, P.; Alcaro, S.; Ortuso, F.; Cirilli, R.; La Torre, F.; Cardia, M. C.; Distinto, S. *J. Med. Chem.* **2005**, *48*, 7113; (b) Chimenti, F.; Bolasco, A.; Manna, F.; Secci, D.; Chimenti, P.; Granese, A.; Befani, O.; Turini, P.; Cirilli, R.; La Torre, F.; Alcaro, S.; Ortuso, F.; Langer, T. *Curr. Med. Chem.* **2006**, *13*, 1411; (c) Chimenti, F.; Fioravanti, R.; Bolasco, A.; Manna, F.; Chimenti, P.; Secci, D.; Rossi, F.; Turini, P.; Ortuso, F.; Alcaro, S.; Cardia, M. C. *Eur. J. Med. Chem.* **2008**, *43*, 2262.
- (a) Chimenti, F.; Secci, D.; Bolasco, A.; Chimenti, P.; Granese, A.; Befani, O.; Turini, P.; Alcaro, S.; Ortuso, F. *Bioorg. Med. Chem. Lett.* **2004**, *14*, 3697; (b) Chimenti, F.; Secci, D.; Bolasco, A.; Chimenti, P.; Granese, A.; Carradori, S.; Befani, O.; Turini, P.; Alcaro, S.; Ortuso, F. *Bioorg. Med. Chem. Lett.* **2006**, *16*, 4135; (c) Chimenti, F.; Secci, D.; Bolasco, A.; Chimenti, P.; Bizzarri, B.; Granese, A.; Carradori, S.; Yáñez, M.; Orallo, F.; Alcaro, S.; Ortuso, F. *J. Med. Chem.* **2009**, *52*, 1935.
- (a) Tipton, K. F. *Biochem. J.* **1972**, *128*, 913; (b) Dar, A.; Khan, K. M.; Ateeq, H. S.; Khan, S.; Rahat, S.; Perveen, S.; Supuran, C. T. *J. Enzyme Inhib. Med. Chem.* **2005**, *20*, 269; (c) Binda, C.; Wang, J.; Li, M.; Hubálek, F.; Mattevi, A.; Edmondson, D. E. *Biochemistry* **2008**, *47*, 5616.
- Chimenti, F.; Maccioni, E.; Secci, D.; Bolasco, A.; Chimenti, P.; Granese, A.; Befani, O.; Turini, P.; Alcaro, S.; Ortuso, F.; Cardia, M. C.; Distinto, S. *J. Med. Chem.* **2007**, *50*, 707.
- Chimenti, F.; Maccioni, E.; Secci, D.; Bolasco, A.; Chimenti, P.; Granese, A.; Carradori, S.; Alcaro, S.; Ortuso, F.; Yáñez, M.; Orallo, F.; Cirilli, R.; Ferretti, R.; La Torre, F. *J. Med. Chem.* **2008**, *51*, 4874.
- (a) Chimenti, F.; Carradori, S.; Secci, D.; Bolasco, A.; Chimenti, P.; Granese, A.; Bizzarri, B. *J. Heterocycl. Chem.* **2009**, *46*, 575; (b) Chimenti, F.; Secci, D.; Bolasco, A.; Chimenti, P.; Granese, A.; Carradori, S.; D'Ascenzio, M.; Yáñez, M.; Orallo, F. *Med. Chem. Commun.* **2010**. doi:10.1039/c0md00014k.
- (a) Raciti, G.; Mazzone, P.; Raudino, A.; Mazzone, G.; Cambria, A. *Bioorg. Med. Chem.* **1995**, *3*, 1485; (b) Castelli, F.; Cambria, M. T.; Mazzone, P.; Pignatello, R. *Thermochim. Acta* **1997**, *302*, 143; (c) Cambria, A.; Raudino, A.; Geronikaki, A.; Buemi, G.; Raciti, G.; Mazzone, P.; Guccione, S.; Ragusa, S. *J. Enzyme Inhib.* **1999**, *14*, 307.
- Yáñez, M.; Fraiz, N.; Cano, E.; Orallo, F. *Biochem. Biophys. Res. Commun.* **2006**, *344*, 688.
- Tipton, K. F.; Boyce, S.; O'Sullivan, J.; Davey, G. P.; Healy, J. *Curr. Med. Chem.* **2004**, *11*, 1965.
- Szedlacek, S. E.; Duggleby, R. G. *Methods Enzymol.* **1995**, *249*, 144.
- Gerlach, M.; Riederer, P.; Youdim, M. B. H. *Eur. J. Pharmacol.* **1992**, *226*, 97.
- O'Brien, E. M.; Tipton, K. F.; Meroni, M.; Dostert, P. *J. Neural. Transm. Suppl.* **1994**, *41*, 295.
- Berman, H. M.; Westbrook, J.; Feng, Z.; Gilliland, G.; Bhat, T. N.; Weissig, H.; Shindyalov, I. N.; Bourne, P. E. *Nucleic Acids Res.* **2000**, *28*, 235.
- Maestro ver. 4.1, Schroedinger Inc.: Portland, OR, 1998–2001.
- Kaminski, G.; Friesner, R. A.; Tirado-Rives, J.; Jorgensen, W. L. *J. Phys. Chem. B* **2001**, *105*, 6474.
- Mohamadi, F.; Richards, N. G. J.; Guida, W. C.; Liskamp, R.; Lipton, M.; Caufield, C.; Chang, G.; Hendrickson, T.; Still, W. C. *J. Comput. Chem.* **1990**, *11*, 440.
- Hasel, W.; Hendrickson, T. F.; Still, W. C. *Tetrahedron Comput. Methodol.* **1988**, *1*, 103.
- (a) (a) Glide ver. 4.1, Schroedinger Inc.: Portland, OR, 1998–2001.; (b) Eldridge, M. D.; Murray, C. W.; Auton, T. R.; Paolini, G. V.; Mee, R. P. *J. Comput. Aided Mol. Des.* **1997**, *11*, 425.
- DeLano, W. L. *The PyMOL Molecular Graphics System*; DeLano Scientific: San Carlos, CA, 2002. www.pymol.org.